

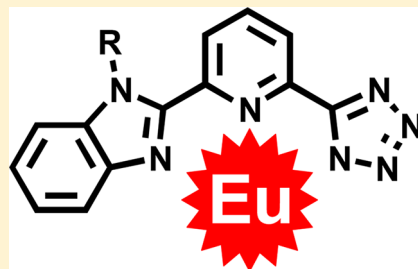
Tridentate Benzimidazole-Pyridine-Tetrazolates as Sensitizers of Europium Luminescence

Nail M. Shavaleev,* Svetlana V. Eliseeva, Rosario Scopelliti, and Jean-Claude G. Bünzli*

École Polytechnique Fédérale de Lausanne, Institut des Sciences et Ingénierie Chimiques, Avenue Forel 2, BCH, CH-1015 Lausanne, Switzerland

Supporting Information

ABSTRACT: We report on new anionic tridentate benzimidazole-pyridine-tetrazolate ligands that form neutral 3:1 complexes with trivalent lanthanides. The ligands are UV-absorbing chromophores that sensitize the red luminescence of europium with energy-transfer efficiency of 74–100%. The lifetime and quantum yield of the sensitized europium luminescence increase from 0.5 ms and 12–13% for the as-prepared solids to 2.8 ms and 41% for dichloromethane solution. From analysis of the data, the as-prepared solids can be described as aqua-complexes $[\text{Ln}(\kappa^3\text{-ligand})_2(\kappa^1\text{-ligand})(\text{H}_2\text{O})_x]$ where the coordinated water molecules are responsible for the strong quenching of the europium luminescence. In solution, the coordinated water molecules are replaced by the nitrogen atoms of the κ^1 -ligand to give anhydrous complexes $[\text{Ln}(\kappa^3\text{-ligand})_3]$ that exhibit efficient europium luminescence. X-ray structures of the anhydrous complexes confirm that the lanthanide ion (La^{III} , Eu^{III}) is nine-coordinate in a distorted tricapped trigonal prismatic environment and that coordination of the lanthanide ion by tetrazolate is weaker than by carboxylate.

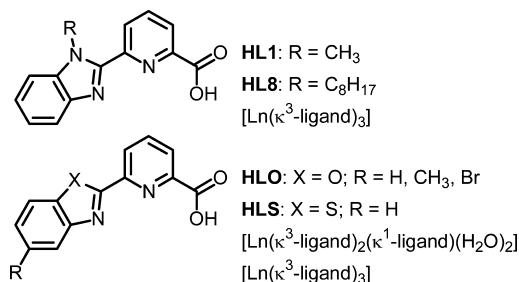


INTRODUCTION

Luminescent lanthanide complexes are seeing an unprecedented surge of interest in view of their applications in lighting, displays, telecommunications, analytical sensors, security inks, anticounterfeiting tags, biomedical imaging, and solar energy conversion.¹ One way of overcoming the problem of faint $f-f$ absorption transitions of the trivalent lanthanide ions to achieve bright luminescence is to surround the lanthanide with organic ligands, which harvest light, transfer the electronic energy to the metal ion, and protect it from nonradiative deactivation.^{1–5}

“Hard” trivalent lanthanides prefer “hard” oxygen ligands, as demonstrated by a recent survey of 1391 crystal structures which showed that 42% of the scrutinized complexes contain exclusively Ln–O bonds while 78% contain at least one Ln–O bond.⁶ In particular, water strongly binds to the lanthanides and strongly quenches their luminescence by nonradiative transfer of electronic energy to high-energy overtones of the O–H vibrational modes.⁷ However, the nature of the donor atom is not the only criterion, and many of the stable lanthanide complexes are made with mixed N,O- or even all-N-donor ligands. For example, “soft” anionic nitrogen ligands that have deprotonated arylamide,⁸ 1,2,3-triazole,⁹ 1,2,4-triazole,¹⁰ or tetrazole^{11–19} metal-binding group(s) were reported to give lanthanide complexes with Ln–N bonds that are stable to air and moisture.

Easy-to-make tetrazole ligands are gaining momentum in d- and f-metal coordination chemistry.^{11–23} Here we test the effect of replacing the “hard” carboxylic acid in benzimidazole-pyridine-2-carboxylates⁴ (Chart 1) by a “soft” tetrazolate (Scheme 1) on the structure and photophysics of lanthanide complexes.

Chart 1. Reference Ligands and Lanthanide Complexes^{3,4}

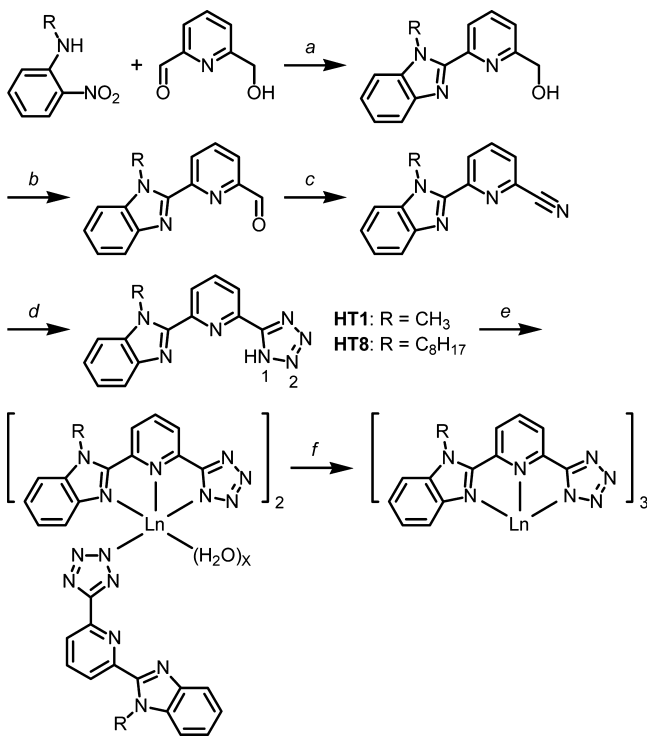
RESULTS AND DISCUSSION

Synthesis. The two new tetrazole ligands, HT1 and HT8, were prepared from 2-carboxaldehyde-6-hydroxymethylpyridine³ and substituted 2-nitroaniline (Scheme 1). The formation of the benzimidazole ring^{4,24} was followed by mild oxidation of the pyridine-2-methanol to the corresponding carboxaldehyde with SeO₂,^{3,4} and by subsequent conversion of the carboxaldehyde into the carbonitrile with NH₂OH·HCl in formic acid²⁵ or in DMSO²⁶ (Supporting Information). Reaction of the carbonitrile with sodium azide in DMF²⁷ gave the target tetrazole ligands as white solids. The ligand HT8 with an *N*-octyl chain was prepared to improve the solubility of the complexes in organic solvents.

Tris-complexes of the ligands with lanthanum and europium, LnT1 and LnT8, were obtained as air- and moisture-stable

Received: February 4, 2014

Published: May 7, 2014

Scheme 1. Synthesis of Ligands and Lanthanide Complexes^a

^aReaction conditions: (a) $\text{Na}_2\text{S}_2\text{O}_4$, 2-methoxyethanol, under N_2 , 110 °C; (b) SeO_2 , dioxane, under N_2 , 110 °C; (c) $\text{NH}_2\text{OH}\cdot\text{HCl}$, sodium formate, formic acid, under N_2 , 120 °C; [alternative] $\text{NH}_2\text{OH}\cdot\text{HCl}$, DMSO, under N_2 , 100 °C; (d) NaN_3 , NH_4Cl , DMF, under N_2 , 110 °C (the numbering of the tetrazole ring is indicated); (e) NaOH (base), $\text{LnCl}_3\cdot n\text{H}_2\text{O}$, ethanol, under air, 65–75 °C; (f) dissolution in CH_2Cl_2 or recrystallization (see text), under air.

white solids from hot ethanol/water solutions with a 3:3:1 molar ratio of ligand, NaOH (base), and $\text{LnCl}_3\cdot n\text{H}_2\text{O}$ (Scheme 1). Elemental analysis indicates that the complexes have the composition $\text{Ln}(\text{ligand})_3\cdot n\text{H}_2\text{O}$, where $n = 2.5\text{--}6$. The structures of the complexes are discussed in the next sections.

Electronic States of the Ligands. The absorption spectra of the ligands HT1 and HT8 display a band centered at ≈ 320 nm with molar absorption coefficient of $(22\text{--}23) \times 10^3 \text{ M}^{-1} \text{ cm}^{-1}$ and with a shoulder at ≈ 330 nm, which correspond to $\pi \rightarrow \pi^*$ transitions of the benzimidazole chromophore (Table 1, Figure 1, and Figures S1 and S2 in the Supporting Information). In the complexes, the absorption maximum of the ligands red-shifts by 2 nm and its intensity increases to $(68\text{--}70) \times 10^3 \text{ M}^{-1} \text{ cm}^{-1}$, reflecting the presence of three

Table 1. Absorption Spectra^a

compound	$\lambda_{\text{max}}/\text{nm}$ ($\epsilon/10^3 \text{ M}^{-1} \text{ cm}^{-1}$)
HT1·0.35H ₂ O	319 (23)
La(T1) ₃ ·6H ₂ O	321 (69), 269 (44)
Eu(T1) ₃ ·3.5H ₂ O	321 (70), 269 (45)
HT8	320 (22)
La(T8) ₃ ·2.5H ₂ O	322 (68), 269 (45)
Eu(T8) ₃ ·3H ₂ O	322 (70), 269 (46)

^aIn DMSO at 250–500 nm; $(1.99\text{--}2.23) \times 10^{-4} \text{ M}$ for the ligands; $(5.30\text{--}6.24) \times 10^{-5} \text{ M}$ for the complexes; at 298 K. Errors: ± 1 nm for λ_{max} ; $\pm 5\%$ for ϵ .

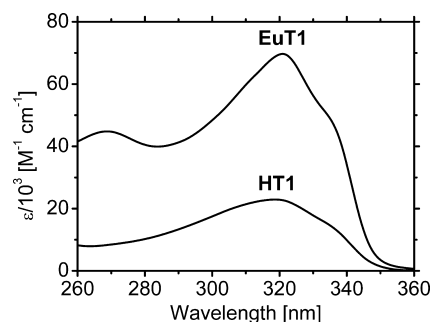


Figure 1. Absorption spectra of ligand HT1·0.35H₂O ($2.23 \times 10^{-4} \text{ M}$) and complex Eu(T1)₃·3.5H₂O ($5.94 \times 10^{-5} \text{ M}$) in DMSO (see also Figures S1 and S2 in the Supporting Information).

coordinated ligands (Table 1, Figure 1, and Figures S1 and S2 in the Supporting Information).

The triplet energy of the ligands (E_T) in lanthanum complexes was determined to be $20.7 \times 10^3 \text{ cm}^{-1}$ from the 0–0 transitions of the phosphorescence spectra, which exhibit ring-breathing vibrational progressions with a spacing of $(1.1\text{--}1.4) \times 10^3 \text{ cm}^{-1}$ (Figure 2 and Table 2). The spectroscopic

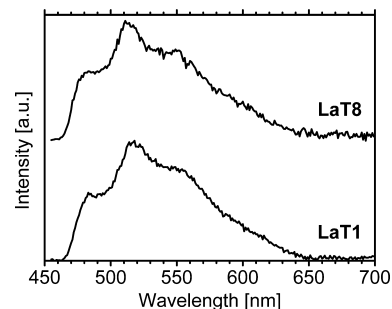


Figure 2. Phosphorescence spectra (corrected and normalized; emission slit: 7 nm) of the as-prepared solid lanthanum complexes at 77 K.

Table 2. Phosphorescence of Solid Lanthanum Complexes^a

complex	$E/10^3 \text{ cm}^{-1}$		
	0–0	0–1	Δ
La(T1) ₃ ·6H ₂ O	20.7	19.3	1.4
La(T8) ₃ ·2.5H ₂ O	20.7	19.6	1.1

^aSee Figure 2. At 77 K. Error: $\pm 200 \text{ cm}^{-1}$.

properties of the ligands HT1 and HT8 are nearly identical, because the ligands differ only by the length of the *N*-alkyl chain; the same statement applies to their complexes.

Europium Luminescence. Upon excitation into the ligand absorption band, the new europium complexes emit red luminescence with a characteristic line-like spectrum^{3–5} in the range 575–710 nm due to the metal-centered $^5\text{D}_0 \rightarrow ^7\text{F}_J$ ($0 \rightarrow J$, $J = 0\text{--}4$) transitions (Figure 3). The emission lines are sharp for the as-prepared solids but are broader for the dichloromethane solution (Figure 3). The $0 \rightarrow 0$ and $0 \rightarrow 3$ transitions are weak: $<0.3\%$ and $<3\%$ of the total emission intensity, respectively (Table S1 in the Supporting Information). The contributions of the $0 \rightarrow 1$, $0 \rightarrow 2$, and $0 \rightarrow 4$ transitions are 19–22%, 42–45%, and 33%, respectively, for the as-prepared solid complexes **EuT1** and **EuT8**, and 22%, 38%, and 38% for

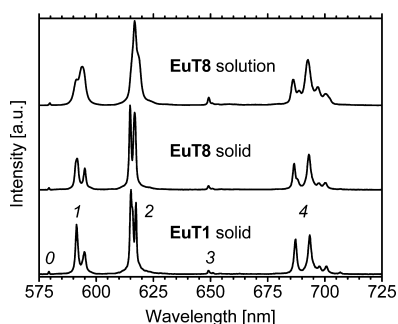


Figure 3. Corrected and normalized luminescence spectra of the europium complexes displaying the ${}^5D_0 \rightarrow {}^7F_{0-4}$ transitions in the as-prepared solid and in 7.5×10^{-4} M solution in CH_2Cl_2 . $\lambda_{\text{exc}} = 355$ nm. Emission slit: 0.2 nm. $T = 298$ K.

EuT8 in dichloromethane solution (Table S1 in the Supporting Information).

High resolution excitation scans over the ${}^5D_0 \rightarrow {}^7F_0$ transition of the as-prepared solid **EuT1** and **EuT8** at 298 K exhibit one sharp line at 17233 and 17232 cm^{-1} with full width at half height of 3 and 5 cm^{-1} , respectively, indicating the presence of a single coordination environment for the europium ion (Figure 4 and Table 3).

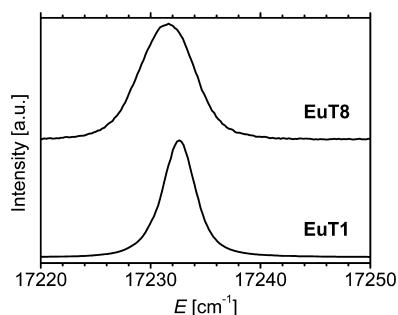


Figure 4. High resolution excitation spectra of the ${}^5D_0 \leftarrow {}^7F_0$ transition of the as-prepared solid europium complexes at 298 K. The emission was monitored at the ${}^5D_0 \rightarrow {}^7F_2$ transition at 610–620 nm.

The emission spectra are independent of the excitation wavelength. Energy transfer from the ligands to the europium²⁸ is confirmed by the excitation spectra, which display onsets corresponding to the ligand absorption (Figures S3 and S4 in the Supporting Information; the excitation spectra were recorded on optically thick samples and, therefore, exhibit saturated signal at $\lambda < 375$ nm). In addition, we observe faint sharp lines at 395 and 463 nm of the ${}^5L_6 \leftarrow {}^7F_{0,1}$ and ${}^5D_2 \leftarrow {}^7F_{0,1}$ f–f transitions of Eu^{III} .²⁹ The weak intensity of the f–f transitions with respect to the ligand bands confirms an antenna effect. Indeed, the energy gaps between the triplet state

of the ligands (energy donor;²⁸ 20 700 cm^{-1} , Table 2) and the $\text{Eu}({}^5D_1)$ levels ($J = 0$, 17 230 cm^{-1} ; $J = 1$, 19 000 cm^{-1})²⁹ are 3470 and 1700 cm^{-1} , respectively, and are adequate for ligand-to-europium energy transfer without much back-transfer.²⁸ In contrast, the $\text{Eu}({}^3D_2)$ level, at 21 600 cm^{-1} ,²⁹ lies above the triplet of the ligands and is probably not involved in the energy transfer.

The observed luminescence decays (τ_{obs} , Table 3) for all of the complexes are single exponential functions in all media at both 298 K and 10 K, indicating the presence of one emissive europium center in each case. The lifetimes increase by less than 10% in going from 298 K to 10 K, which points to the absence of thermally activated deactivation pathways, such as those induced by ligand-to-europium charge-transfer states³⁰ or by back europium-to-ligand energy transfer²⁸ (Table 3).

For the as-prepared solid complexes **EuT1** and **EuT8**, the luminescence lifetimes are short, around 0.5 ms, and the measured quantum yields of the ligand-sensitized europium luminescence (Q_L^{Eu}) are only 12–13%. In contrast, when **EuT8** is dissolved into dichloromethane, both the lifetime and the quantum yield increase considerably to $\tau_{\text{obs}} = 2.8$ ms and $Q_L^{\text{Eu}} = 41\%$ (Table 3). To explain these results, we postulate that the as-prepared solids are aqua-complexes $[\text{Ln}(\kappa^3\text{-ligand})_2(\kappa^1\text{-ligand})(\text{H}_2\text{O})_x] \cdot y\text{H}_2\text{O}$, where one of the tetrazolate ligands is κ^1 -bound and where water molecules (probably two, as indicated by the short lifetime of 0.5 ms)³ are coordinated to the europium ion (Scheme 1), inducing a strong luminescence quenching. Thermogravimetric analysis supports this interpretation: the as-prepared solid **LnT8** undergo a weight loss in the range 30–100 °C corresponding to 0.2–0.4 outer-sphere water molecules and another one between 100–180 °C corresponding to 1.85 coordinated water molecules (Figure S5 and Table S2 in the Supporting Information). In dichloromethane, a noncoordinating solvent, the lanthanide-bound water molecules are probably replaced by the benzimidazole and pyridine nitrogen atoms of the κ^1 -ligand to give the anhydrous complex $[\text{Ln}(\kappa^3\text{-ligand})_3]$, which exhibits higher luminescence efficiency (Scheme 1 and Figure 5). Evaporation of dichloromethane solution gives a solid that exhibits a biexponential luminescence decay at 10 K with two lifetimes that correspond to the aqua (0.55 ms) and the anhydrous (2.43 ms) complexes, indicating reversible conversion between these two species³ (in general, lanthanide–ligand bonds are ionic and, therefore, nondirectional and labile¹).

More insight into the photophysics of the complexes can be gained by analyzing the data in terms of eq 1, where Q_L^{Eu} and $Q_{\text{Eu}}^{\text{Eu}}$ are ligand-sensitized and intrinsic luminescence quantum yields of the $\text{Eu}({}^5D_0)$ level, η_{sens} is the efficiency of ligand-to-europium energy transfer, and τ_{obs} and τ_{rad} are the observed and radiative lifetimes of $\text{Eu}({}^5D_0)$:

$$Q_L^{\text{Eu}} = \eta_{\text{sens}} \times Q_{\text{Eu}}^{\text{Eu}} = \eta_{\text{sens}} \times (\tau_{\text{obs}}/\tau_{\text{rad}}) \quad (1)$$

Table 3. Photophysics of Europium Complexes^a

complex		ν_{0-0}/cm^{-1}	$Q_L^{\text{Eu}}/\%$	$\tau_{\text{obs}}/\text{ms}$		$\tau_{\text{rad}}/\text{ms}$	$Q_{\text{Eu}}^{\text{Eu}}/\%$	$\eta_{\text{sens}}/\%$
				298 K	10 K			
Eu(T1) ₃ ·3.5H ₂ O	solid	17233(3) ^b	12	0.51	0.47	4.36	12	100
Eu(T8) ₃ ·3H ₂ O	solid	17232(5) ^b	13	0.52	0.5	3.93	13	100
	CH ₂ Cl ₂		41	2.83		5.09	56	74

^aAt 298 K, unless stated otherwise. $\lambda_{\text{exc}} = 355$ nm. Errors: τ_{obs} , $\pm 2\%$; Q_L^{Eu} , $\pm 10\%$; τ_{rad} , $\pm 10\%$; $Q_{\text{Eu}}^{\text{Eu}}$, $\pm 12\%$; η_{sens} , $\pm 22\%$. ^bSee Figure 4. Full width at half height in parentheses.

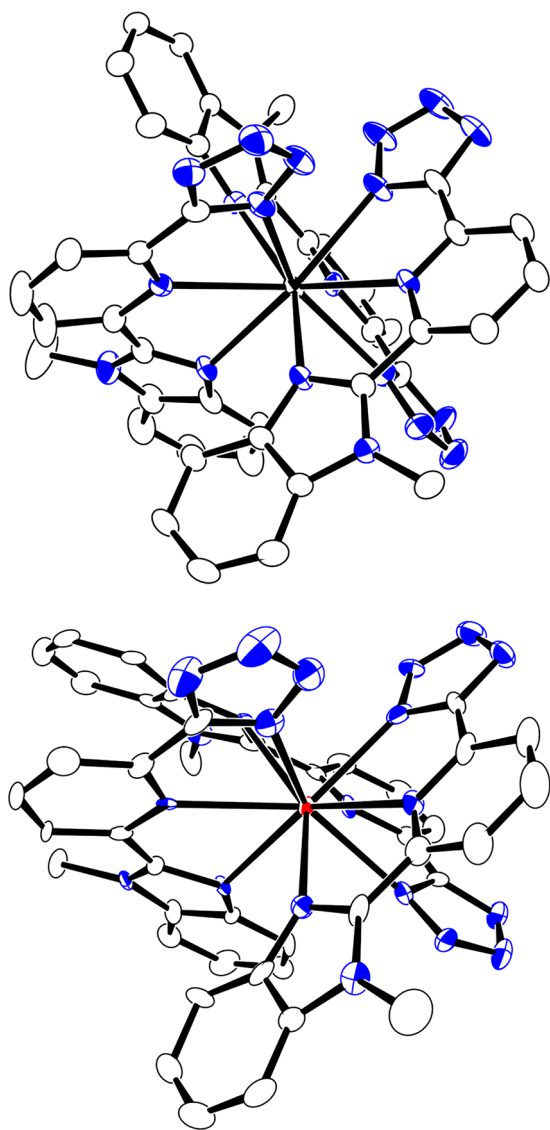


Figure 5. Structures of complexes $[\text{Ln}(\kappa^3\text{-T1})_3]$ ($\text{Ln} = \text{La}$, top; Eu , bottom) (50% probability ellipsoids; H atoms and cocrystallized solvent molecules omitted; ORTEP). Heteroatoms: N, blue; La, black; $\text{Eu}(\text{I})$, red.

In a highly luminescent lanthanide complex, the ligands must protect the metal ion from nonradiative deactivation (parameter $Q_{\text{Eu}}^{\text{Eu}}$) and must provide efficient light harvesting and energy transfer (parameter η_{sens}). The radiative lifetime of $\text{Eu}({}^5\text{D}_0)$ was calculated from eq 2,^{31,32} where n is the refractive index (taken as 1.5 for solid-state metal–organic complexes^{3,4} or 1.4242 for the CH_2Cl_2 solution), A_{MD} is the spontaneous emission probability for the ${}^5\text{D}_0 \rightarrow {}^7\text{F}_1$ transition in vacuo (14.65 s^{-1}), and $I_{\text{tot}}/I_{\text{MD}}$ is the ratio of the integrated emission intensity of the total corrected europium spectrum to that of the magnetic dipole ${}^5\text{D}_0 \rightarrow {}^7\text{F}_1$ transition (Table S1 in the Supporting Information):

$$1/\tau_{\text{rad}} = A_{\text{MD}} \times n^3 \times (I_{\text{tot}}/I_{\text{MD}}) \quad (2)$$

The radiative lifetimes for the as-prepared solid complexes **EuT1** and **EuT8** are 4.36 and 3.93 ms, respectively. When **EuT8** is dissolved in dichloromethane, one anticipates a lengthening of τ_{rad} to 4.59 ms due to the decrease in refractive index (eq 2). In the experiment, however, a longer radiative

lifetime is found, 5.09 ms, indicating that the inner coordination sphere of the lanthanide ion changes upon dissolution of the complex.

The intrinsic quantum yield of europium could not be determined upon direct $f-f$ excitation because of the low intensity of the $f-f$ absorption. Instead, it was calculated from the ratio $Q_{\text{Eu}}^{\text{Eu}} = \tau_{\text{obs}}/\tau_{\text{rad}}$ to be 12–13% for the as-prepared solid and 56% for the solution (Table 3). The higher luminescence efficiency of the complex in dichloromethane solution confirms that water molecules are not coordinated to the europium in the solution and that the tetrazolate ligands efficiently protect the excited europium ion from nonradiative deactivation. However, the calculated efficiency of ligand-to-europium energy transfer, $\eta_{\text{sens}} = Q_{\text{L}}^{\text{Eu}}/Q_{\text{Eu}}^{\text{Eu}}$, decreases from 100% in the as-prepared solid to 74% in the solution because of energy losses within the ligands induced by collisions with solvent molecules and by labile bonding with europium (Table 3). Nevertheless, these losses are compensated by the large increase in $Q_{\text{Eu}}^{\text{Eu}}$ in the solution.

Structure of Anhydrous Complexes. Small-scale recrystallization (<2 mg) of the as-prepared aqua-complexes from boiling organic solvent gave upon cooling anhydrous complexes $[\text{Ln}(\kappa^3\text{-T1})_3] \cdot 3\text{CH}_3\text{CN}$ and $[\text{Eu}(\kappa^3\text{-T1})_3] \cdot 2.25\text{C}_2\text{H}_5\text{OH}$ as the only single crystals suitable for structural characterization that we could isolate (see Table S3 and the Supporting Information for details).

The two complexes have similar structural properties (Figure 5 and Table 4; the structure of $[\text{Eu}(\kappa^3\text{-T1})_3]$ contains two independent molecules). The lanthanide ion is nine-coordinate. It is bound to three tridentate ligands, and its coordination polyhedron is a distorted tricapped trigonal prism (TCTP), with the N(py = pyridine) atoms in capping positions and in-plane with Ln^{III} . Two triangular faces of the prism are defined by N(tz)–N(b)–N(b) and N(tz)–N(tz)–N(b) atoms (tz = tetrazolate, b = benzimidazole). Each of the three ligands connects the triangular faces of the TCTP via a capping position. The ligands are arranged “up–up–down” around the lanthanide, resulting in a low symmetry (formally C_1) of the complex.

The coordinated ligands are not planar. The dihedral angles between tetrazolate and pyridine are 4–10°. The angles between pyridine and benzimidazole are larger, with a wider range of 11–40° (Table 4). The three ligands in the complex are not equally strongly bonded to the lanthanide as reflected in the bond lengths. For a given ligand, the lanthanide–benzimidazole bond is often the longest one with the widest variation (Table 4). The bond lengths decrease from La^{III} to Eu^{III} because of the lanthanide contraction.

Cocrystallized ethanol molecules in the structure of $[\text{Eu}(\kappa^3\text{-T1})_3]$ form hydrogen bonds with N2 or N3 atoms of the tetrazolate with $\text{N}\cdots\text{O}$ distances of 2.93(1)–3.03(3) Å. Inter-lanthanide communication is negligible, with $\text{Ln}–\text{Ln}$ distances >9.9 Å, which minimizes concentration quenching, a favorable condition for efficient luminescence.

The bonding strengths of the ligands were quantified by the bond-valence method,³³ wherein a donor atom j at a distance $d_{\text{Ln},j}$ from the metal ion is characterized by a bond-valence contribution $\nu_{\text{Ln},j}$:

$$\nu_{\text{Ln},j} = e^{(R_{\text{Ln},j} - d_{\text{Ln},j})/b} \quad (3)$$

where $R_{\text{Ln},j}$ are the bond-valence parameters for the pair of interacting atoms ($\text{La}–\text{N}$, 2.261 Å; $\text{Eu}–\text{N}$, 2.161 Å),³⁴ and b is

Table 4. Structural Parameters^a

complex	bond lengths ^b (Å)			angles ^{b,c} (deg)		Ln–Ln ^d (Å)
	Ln–N(tz)	Ln–N(py)	Ln–N(b)	tz–py	py–b	
[La(κ^3 -T1) ₃]	2.607(2)	2.708(2)	2.660(2)	4.07	11.25	9.9243(6)
	2.618(2)	2.700(2)	2.710(2)	4.84	27.23	
	2.620(2)	2.694(2)	2.686(2)	4.40	25.66	
	2.615(11)	2.701(11)	2.685(41)	4.4(6)	21(14)	
	<i>0.013</i>	<i>0.014</i>	<i>0.050</i>	<i>0.77</i>	<i>16</i>	
[Eu(κ^3 -T1) ₃] (1)	2.481(9)	2.604(8)	2.565(8)	5.37	10.58	10.2890(10)
	2.501(8)	2.556(8)	2.669(8)	7.94	34.25	
	2.521(8)	2.616(7)	2.630(8)	8.64	21.39	
	2.501(33)	2.592(52)	2.621(86)	7(3)	22(19)	
	<i>0.040</i>	<i>0.060</i>	<i>0.104</i>	<i>3.3</i>	<i>24</i>	
[Eu(κ^3 -T1) ₃] (2)	2.502(9)	2.549(8)	2.658(9)	5.04	39.76	
	2.506(9)	2.574(8)	2.564(8)	9.52	27.24	
	2.538(8)	2.601(7)	2.571(8)	6.80	11.56	
	2.515(32)	2.575(42)	2.598(86)	7(4)	26(23)	
	<i>0.036</i>	<i>0.052</i>	<i>0.094</i>	<i>4.5</i>	<i>28</i>	

^aEach row corresponds to one ligand. Numbers in bold are averaged data with standard deviations 2σ . Numbers in bold and in italic are differences between the minimum and the maximum values. ^btz = tetrazole; py = pyridine; b = benzimidazole. ^cThe dihedral angles between the planes of tetrazole and pyridine or pyridine and benzimidazole. ^dMinimum Ln–Ln distance.

a constant (0.37 Å). The bond valence sum (BVS) of the metal ion V_{Ln} (eq 4) is supposed to match its oxidation state if average bonds are standard:

$$V_{Ln} = \sum_j \nu_{Ln,j} \quad (4)$$

The BVS for the new structures (3.02–3.10) are close to the expected value for Ln^{III} (3.00 ± 0.25) and confirm the good quality of the crystallographic data (Table 5). The average contributions from the coordinating groups are in the expected order: N(tz), 0.39(3) > N(py), 0.31(4) > N(b), 0.31(7) (Table 5).^{3,4}

Table 5. Calculated Bond Valence Parameters

complex	V_{Ln}	$\nu_{Ln,j}(N)^a$		
		N(tz)	N(py)	N(b)
[La(κ^3 -T1) ₃]	3.02	0.38(1)	0.30(1)	0.32(4)
[Eu(κ^3 -T1) ₃] (1)	3.01	0.40(4)	0.31(5)	0.29(8)
[Eu(κ^3 -T1) ₃] (2)	3.06	0.38(4)	0.33(5)	0.31(8)
all data		0.39(3)	0.31(4)	0.31(7)

^aAveraged over three ligand bond-valence contributions with standard deviation 2σ .

Structure of Aqua-Complexes. The postulated aqua-complexes (Scheme 1) likely resemble the previously reported nine-coordinate lanthanide aqua-carboxylates [Ln(κ^3 -ligand)₂(κ^1 -ligand)(H₂O)₂] with deprotonated tridentate ligands HLO and HLS (Chart 1).³ These aqua-carboxylates exhibit europium luminescence in solid state with $\tau_{obs} = 0.42$ – 0.47 ms and $Q_{T}^{Eu} = 12$ – 14% that are close to those of the aqua-tetrazolate complexes reported here. Moreover, these aqua-carboxylates can be converted into the anhydrous complexes [Ln(κ^3 -ligand)₃] on recrystallization.³

The tautomeric tetrazolate heterocycle can bind to a lanthanide ion by either the N1 or the N2 atom: we observe N1-coordination for the κ^3 -ligand (Figure 5) and we postulate N2-coordination, for steric reasons, for the κ^1 -ligand (Scheme 1). We note that chelating tetrazolate ligands are known, in

certain cases, to bind lanthanides by monodentate N1- or N2-coordination, instead of by chelation, or even to be replaced by water to become noncoordinated counteranions.^{18–20}

Tetrazolate versus Carboxylate. We previously reported lanthanide complexes with carboxylate analogues HL1 and HL8 of the new tetrazolate ligands (Chart 1).⁴ In contrast to the tetrazolates, which give aqua-complexes, these carboxylates, under identical conditions, give anhydrous complexes [Ln(κ^3 -ligand)₃] that exhibit efficient europium luminescence in the solid state and in solution, with $\tau_{obs} = 2.46$ – 2.95 ms and $Q_{T}^{Eu} = 52$ – 71% .⁴ Therefore, “hard” carboxylates are better ligands and sensitizers for lanthanides than are “soft” tetrazolates.

The structure of the anhydrous tetrazolate complexes (Figure 5) is similar to that of the anhydrous carboxylates.⁴ However, the average Ln–N(benzimidazole) bond in [Ln(κ^3 -T1)₃] is shorter by 0.058–0.083 Å and its bond-valence contribution is larger by 0.04–0.06 than in [Ln(κ^3 -L1)₃]. It is a result of a weaker binding of the lanthanide by the N1-tetrazolate vs the O-carboxylate which have the corresponding average bond-valence contribution of 0.39 vs 0.42 (Figure 5 and Tables 4 and 5).

In the ligands, replacing carboxylic acid by tetrazole red-shifts the lowest-energy absorption by <5 nm but does not change its intensity (Table 1; for HL1 and HL8, $\lambda_{max} \approx 315$ nm and $\epsilon = 22 \times 10^3$ M⁻¹ cm⁻¹).⁴ In the complexes, replacing carboxylate by tetrazolate enhances the intensity of the lowest-energy absorption but does not shift its maximum and does not change the triplet state energy of the ligand (Tables 1–3; for [Ln(κ^3 -L1)₃] and [Ln(κ^3 -L8)₃], $\lambda_{max} = 316$ – 321 nm, $\epsilon = (51$ – $59) \times 10^3$ M⁻¹ cm⁻¹ and $E_T = (20.2$ – $21.1) \times 10^3$ cm⁻¹).⁴

In comparison to the tetrazolate ligand in [Eu(κ^3 -T8)₃], the carboxylate ligand in [Eu(κ^3 -L8)₃] transfers energy to the europium more efficiently ($\eta_{sens} = 74\%$ vs 83%) and protects the europium against nonradiative deactivations better ($Q_{T}^{Eu} = 56\%$ vs 63%) to give a higher ligand-sensitized quantum yield in solution ($Q_{T}^{Eu} = 41\%$ vs 52%) (Table 3).⁴ These differences come from the higher affinity of the lanthanides for the “hard” carboxylate than for the “soft” tetrazolate.

In the solid state, the radiative lifetimes of the aqua-tetrazolate complexes, 4.36 and 3.93 ms (Table 3), are longer

than are those reported for the aqua-carboxylates $[\text{Ln}(\kappa^3\text{-LO})_2(\kappa^1\text{-LO})(\text{H}_2\text{O})_2]$ and $[\text{Ln}(\kappa^3\text{-LS})_2(\kappa^1\text{-LS})(\text{H}_2\text{O})_2]$, 3.2–3.5 ms,³ and shorter than are those for the anhydrous carboxylates $[\text{Eu}(\kappa^3\text{-L1})_3]$ and $[\text{Eu}(\kappa^3\text{-L8})_3]$, 4.60–4.7 ms (Chart 1).⁴ In solution, the radiative lifetime of $[\text{Eu}(\kappa^3\text{-T8})_3]$, 5.09 ms, is longer than that of $[\text{Eu}(\kappa^3\text{-L8})_3]$, 4.39 ms,⁴ which may be explained by a more symmetric coordination environment of the Eu^{III} in the anhydrous tetrazolate than in the anhydrous carboxylate, that is, N_9 vs N_6O_3 donor atom set, and by a weaker binding and, therefore, weaker perturbation of the metal *f*-orbitals by tetrazolate than by carboxylate.

Fine structure of high-resolution luminescence spectra of the europium ion, especially when they are recorded for single crystals at low temperature, can provide information³⁵ on the coordination environment of Eu^{III} . The $0 \rightarrow 1$ luminescence transition of the new europium tetrazolate complexes exhibits three bands (two of which nearly coincide) for the as-prepared polycrystalline solid aqua-complex or two very broad bands for the solution of anhydrous complex (Figure 3). These luminescence spectra, together with the structural formulas (Scheme 1), suggest that the local symmetry³⁵ around the Eu^{III} is likely to be close to C_1 (as-prepared solid) or pseudo- C_3 (solution).

CONCLUSIONS

Anionic tridentate benzimidazole-pyridine-tetrazolates are a new class of “soft” nitrogen chromophore ligands³⁶ that can be coordinated to lanthanide^{11–19} and actinide^{13,21} *f*-metals and to octahedral and square-planar *d*-metals^{13,23} to give luminescent and redox-active complexes. The ligands form neutral complexes with lanthanum and europium and efficiently sensitize the red luminescence of europium. Although coordination of lanthanide ions by tetrazolate is weaker than by carboxylate, tetrazolates are promising antenna ligands for sensitizing lanthanide luminescence, and further modification should be able to enhance their coordination properties. In addition, “soft” nitrogen ligands are applied for lanthanide/actinide separation in nuclear fuel reprocessing,³⁷ and the tetrazole ligands, in neutral or anion form, may be of interest in that area of research.

EXPERIMENTAL SECTION

General Information. Elemental analyses were performed by Dr. E. Solari, Service for Elemental Analysis, Institute of Chemical Sciences and Engineering (EPFL). ¹H and ¹³C NMR spectra were recorded on Bruker Avance DRX 400 MHz and Bruker Avance II 800 MHz spectrometers.

Chemicals from commercial suppliers were used without purification. Chromatography was performed on a column with an i.d. of 30 mm on silica gel 60 (Fluka, Nr 60752). The progress of reactions and the elution of products were followed on TLC plates (silica gel 60 F₂₅₄ on aluminum sheets, Merck).

Absorption spectra in the range 250–500 nm were measured on a PerkinElmer Lambda 900 UV/vis/NIR spectrometer. Luminescence spectra were recorded on a Horiba-Jobin Yvon Fluorolog FL 3-22 spectrometer and were corrected for the instrumental function. Quantum yields were determined on the same instrument by an absolute method with a modified homemade integrating sphere.³² Luminescence lifetimes were measured with a previously described instrumental setup.^{3,4} Spectroscopic studies were conducted in optical cells of 2 mm path length or in 2 mm i.d. quartz capillaries under air. The solutions in CH_2Cl_2 (Fisher Scientific, analytical reagent grade) were freshly prepared before each experiment.

CAUTION: Tetrazole derivatives and other nitrogen-rich heterocycles are known to be an explosive hazard.³⁸ We did not encounter

any problems in the everyday handling of small quantities of the new tetrazole ligands and tetrazolate complexes; however, we did not perform stress tests on these materials.

Synthesis of Ligands. The reactions were performed under nitrogen (Scheme 1).²⁵ Substituted 2-pyridinecarbonitrile (Supporting Information), NaN_3 (**CAUTION:** explosive hazard, toxic; small excess, Fluka), and NH_4Cl (small excess) were stirred in dry degassed DMF (2.5 mL, absolute, puriss >99.8% GC, over molecular sieves, Fluka) at 110 °C (bath temperature) for 24 h to give a yellow suspension. Water (20–30 mL) was added. The pH of the resulting suspension was adjusted to pH 3–4. It was stirred for 1 h at room temperature. The solid was filtered, washed with solvents (specified below), and dried under vacuum to give the pure product. If necessary, the ligands can be purified by chromatography (silica, $\text{CH}_3\text{OH}/\text{CH}_2\text{Cl}_2$). They are soluble in DMSO and in mixtures of $\text{CH}_2\text{Cl}_2/\text{CH}_3\text{OH}$. Freshly prepared samples are also soluble in CH_2Cl_2 . Further details are provided below.

HT1-0.35H₂O. The reaction was performed with substituted 2-pyridinecarbonitrile (Supporting Information, 385 mg, 1.64 mmol), NaN_3 (118 mg, 1.82 mmol), and NH_4Cl (97 mg, 1.81 mmol). The product was washed with water and ether/hexane (1:1). White solid: 420 mg (1.48 mmol; 90%). Anal. Calcd for $\text{C}_{14}\text{H}_{11}\text{N}_7 \cdot 0.35\text{H}_2\text{O}$ (MW 283.59): C, 59.29; H, 4.16; N, 34.57. Found: C, 58.96; H, 4.13; N, 35.03. ¹H NMR (400 MHz, DMSO-*d*₆): δ = 8.46 (d, *J* = 8.0 Hz, 1H), 8.33 (d, *J* = 7.6 Hz, 1H), 8.27 (t, *J* = 8.0 Hz, 1H), 7.80–7.71 (m, 2H), 7.38 (t, *J* = 7.6 Hz, 1H), 7.31 (t, *J* = 7.6 Hz, 1H), 4.31 (s, 3H) ppm; NH proton not observed. ¹³C NMR (200 MHz, DMSO-*d*₆): δ = 155.2, 150.9, 149.4, 143.6, 142.3, 139.8, 137.5, 126.9, 124.0, 123.5, 123.1, 120.0, 111.5, 33.3 ppm. ESI⁺ TOF MS: *m/z* 278.2 {M + H}⁺.

HT8. The reaction was performed with substituted 2-pyridinecarbonitrile (Supporting Information, 584 mg, 1.76 mmol), NaN_3 (126 mg, 1.94 mmol), and NH_4Cl (103 mg, 1.93 mmol). The product was washed with water and hexane. White solid: 604 mg (1.61 mmol; 91%). Anal. Calcd for $\text{C}_{21}\text{H}_{23}\text{N}_7$ (MW 375.47): C, 67.18; H, 6.71; N, 26.11. Found: C, 67.06; H, 6.74; N, 26.16. ¹H NMR (400 MHz, DMSO-*d*₆): δ = 8.44 (dd, *J* = 7.6, 1.2 Hz, 1H), 8.30 (dd, *J* = 7.6, 1.2 Hz, 1H), 8.25 (t, *J* = 7.6 Hz, 1H), 7.79–7.71 (m, 2H), 7.36 (t, *J* = 7.6 Hz, 1H), 7.30 (t, *J* = 7.6 Hz, 1H), 4.98 (t, *J* = 7.2 Hz, 2H), 1.70–1.58 (m, 2H), 1.19–0.92 (m, 10H), 0.74 (t, *J* = 7.2 Hz, 3H) ppm; NH proton not observed. ¹³C NMR (200 MHz, DMSO-*d*₆): δ = 155.9, 151.2, 149.1, 144.0, 142.6, 139.8, 136.9, 126.7, 124.0, 123.6, 123.0, 120.2, 111.6, 44.9, 31.4, 30.0, 28.9, 28.7, 26.3, 22.4, 14.3 ppm. ESI⁺ TOF MS: *m/z* 376.3 {M + H}⁺.

Synthesis of Complexes. The reactions were performed under air with a 3:3:1 molar ratio of the ligand, NaOH (base), and $\text{LnCl}_3 \cdot n\text{H}_2\text{O}$ (Scheme 1). The ligand was suspended in hot ethanol (65–75 °C, 5 mL; the same temperature was kept throughout the reaction). A solution of NaOH in water was added (0.5–1 mL, used as a stock solution with 100 mg of NaOH per 10 mL of water). The mixture was stirred for 10 min to give a colorless solution. A solution of $\text{LnCl}_3 \cdot n\text{H}_2\text{O}$ (*n* = 6 or 7; 99.9%, Aldrich) in water (2 mL) was added dropwise over 5 min. The mixture was stirred for further 5 min. Usually, a white precipitate of the complex appeared on stirring. However, if it was required, an additional volume of water (specified below) was added to induce and complete precipitation of the complex. The resulting suspension was stirred for 5 min at 65–75 °C. It was allowed to cool to 40–50 °C. It was filtered while it was warm. The product was washed with ethanol/water (1:1) and ether (**LnT1**) or hexane (**LnT8**). It was dried under vacuum at room temperature. The complexes are soluble in DMSO, boiling ethanol, and boiling acetonitrile. They are insoluble in hexane and water. **LnT1** are insoluble in CH_2Cl_2 at room temperature. Freshly prepared **LnT8** are soluble in CH_2Cl_2 at room temperature up to 1 mg/mL, although dissolution is slow and takes up to 24 h to complete. Aged solid samples of **LnT8** (>1 month) do not dissolve completely in CH_2Cl_2 . Further details are provided below.

La(T1)₃·6H₂O. The complex precipitated on addition of water (2 mL) and cooling. White solid: 38 mg (0.035 mmol, 60%) from HT1·0.35H₂O (50 mg, 0.176 mmol), NaOH (7.05 mg, 0.176 mmol), and $\text{LaCl}_3 \cdot 7\text{H}_2\text{O}$ (21.8 mg, 0.059 mmol). Anal. Calcd for $\text{C}_{42}\text{H}_{30}\text{LaN}_{21}$

6H₂O (MW 1075.83): C, 46.89; H, 3.93; N, 27.34. Found: C, 46.93; H, 4.02; N, 27.25.

La(T8)₃·2.5H₂O. The complex was precipitated with water (1 mL). White solid: 39 mg (0.030 mmol, 68%) from HT8 (50 mg, 0.133 mmol), NaOH (5.33 mg, 0.133 mmol), and LaCl₃·7H₂O (16.5 mg, 0.044 mmol). Anal. Calcd for C₆₃H₇₂LaN₂₁·2.5H₂O (MW 1307.33): C, 57.88; H, 5.94; N, 22.50. Found: C, 57.74; H, 5.86; N, 22.60.

Eu(T1)₃·3.5H₂O. The complex precipitated on addition of water (2 mL) and cooling. White solid: 46 mg (0.044 mmol, 75%) from HT1·0.35H₂O (50 mg, 0.176 mmol), NaOH (7.05 mg, 0.176 mmol), and EuCl₃·6H₂O (21.5 mg, 0.059 mmol). Anal. Calcd for C₄₂H₃₀EuN₂₁·3.5H₂O (MW 1043.85): C, 48.33; H, 3.57; N, 28.18. Found: C, 48.45; H, 3.72; N, 27.75.

Eu(T8)₃·3H₂O. The complex was precipitated with water (1 mL). White solid: 50 mg (0.038 mmol, 85%) from HT8 (50 mg, 0.133 mmol), NaOH (5.33 mg, 0.133 mmol), and EuCl₃·6H₂O (16.3 mg, 0.044 mmol). Anal. Calcd for C₆₃H₇₂EuN₂₁·3H₂O (MW 1329.40): C, 56.92; H, 5.91; N, 22.13. Found: C, 56.66; H, 5.84; N, 22.45. To check reproducibility, we prepared a second batch of the complex by the same procedure: 49 mg (0.037 mmol, 84%). Anal. Calcd for C₆₃H₇₂EuN₂₁·3H₂O (MW 1329.40): C, 56.92; H, 5.91; N, 22.13. Found: C, 57.22; H, 5.76; N, 22.30. The photophysical properties of the two batches were identical.

■ ASSOCIATED CONTENT

Supporting Information

Synthesis of precursors; absorption, luminescence, and ¹H NMR spectra; crystallographic data; CIF of the crystal structures, CCDC 983483 and 983484. This material is available free of charge via the Internet at <http://pubs.acs.org>.

■ AUTHOR INFORMATION

Corresponding Authors

*Tel: +41 21 693 9821. Fax: +41 21 693 5550. E-mail: shava@mail.ru.

*E-mail: jean-claude.bunzli@epfl.ch.

Notes

The authors declare no competing financial interest.

■ ACKNOWLEDGMENTS

This project was supported by the Swiss National Science Foundation (grant 200020_119866/1).

■ REFERENCES

- (1) (a) Eliseeva, S. V.; Bünzli, J.-C. G. *Chem. Soc. Rev.* **2010**, *39*, 189–227. (b) Bünzli, J.-C. G.; Eliseeva, S. V. *Chem. Sci.* **2013**, *4*, 1939–1949.
- (2) (a) Armelao, L.; Quici, S.; Barigelletti, F.; Accorsi, G.; Bottaro, G.; Cavazzini, M.; Tondello, E. *Coord. Chem. Rev.* **2010**, *254*, 487–505. (b) Katkova, M. A.; Bochkarev, M. N. *Dalton Trans.* **2010**, *39*, 6599–6612. (c) Reddy, M. L. P.; Sivakumar, S. *Dalton Trans.* **2013**, *42*, 2663–2678.
- (3) Shavaleev, N. M.; Scopelliti, R.; Gummy, F.; Bünzli, J.-C. G. *Inorg. Chem.* **2009**, *48*, 6178–6191.
- (4) (a) Shavaleev, N. M.; Gummy, F.; Scopelliti, R.; Bünzli, J.-C. G. *Inorg. Chem.* **2009**, *48*, 5611–5613. (b) Shavaleev, N. M.; Eliseeva, S. V.; Scopelliti, R.; Bünzli, J.-C. G. *Chem.—Eur. J.* **2009**, *15*, 10790–10802.
- (5) (a) D'Aléo, A.; Picot, A.; Beeby, A.; Williams, J. A. G.; Le Guennic, B.; Andraud, C.; Maury, O. *Inorg. Chem.* **2008**, *47*, 10258–10268. (b) Miyata, K.; Hasegawa, Y.; Kuramochi, Y.; Nakagawa, T.; Yokoo, T.; Kawai, T. *Eur. J. Inorg. Chem.* **2009**, 4777–4785. (c) Regueiro-Figueroa, M.; Bensenane, B.; Ruscsák, E.; Esteban-Gómez, D.; Charbonnière, L. J.; Tircsó, G.; Tóth, I.; de Blas, A.; Rodríguez-Blas, T.; Platas-Iglesias, C. *Inorg. Chem.* **2011**, *50*, 4125–4141. (d) Sykes, D.; Tidmarsh, I. S.; Barbieri, A.; Sazanovich, I. V.; Weinstein, J. A.; Ward, M. D. *Inorg. Chem.* **2011**, *50*, 11323–11339.

(e) de Bettencourt-Dias, A.; Barber, P. S.; Bauer, S. *J. Am. Chem. Soc.* **2012**, *134*, 6987–6994. (f) Zaim, A.; Nozary, H.; Guéneé, L.; Besnard, C.; Lemonnier, J.-F.; Petoud, S.; Piguet, C. *Chem.—Eur. J.* **2012**, *18*, 7155–7168.

(6) Huang, C.; Bian, Z. *Rare Earth Coordination Chemistry: Fundamentals and Applications*; Huang, C., Ed.; John Wiley & Sons (Asia): Singapore, 2010; Ch. 1, pp 1–40.

(7) (a) Beeby, A.; Clarkson, I. M.; Dickins, R. S.; Faulkner, S.; Parker, D.; Royle, L.; de Sousa, A. S.; Williams, J. A. G.; Woods, M. *J. Chem. Soc., Perkin Trans.* **1999**, *2*, 493–503. (b) Supkowski, R. M.; Horrocks, W. D., Jr. *Inorg. Chim. Acta* **2002**, *340*, 44–48.

(8) (a) Zebret, S.; Dupont, N.; Bernardinelli, G.; Hamacek, J. *Chem.—Eur. J.* **2009**, *15*, 3355–3358. (b) Zebret, S.; Dupont, N.; Besnard, C.; Bernardinelli, G.; Hamacek, J. *Dalton Trans.* **2012**, *41*, 4817–4823.

(9) Rybak, J.-C.; Meyer, L. V.; Wagenhöfer, J.; Sextl, G.; Müller-Buschbaum, K. *Inorg. Chem.* **2012**, *51*, 13204–13213.

(10) (a) Gusev, A. N.; Shul'gin, V. F.; Meshkova, S. B.; Doga, P. G.; Hasegawa, M.; Aleksandrov, G. G.; Eremenko, I. L.; Linert, W. *Inorg. Chim. Acta* **2012**, *387*, 321–326. (b) Gusev, A. N.; Shul'gin, V. F.; Nishimenko, G.; Hasegawa, M.; Linert, W. *Synth. Met.* **2013**, *164*, 17–21. (c) Gusev, A. N.; Hasegawa, M.; Nishchymenko, G. A.; Shul'gin, V. F.; Meshkova, S. B.; Doga, P.; Linert, W. *Dalton Trans.* **2013**, *42*, 6936–6943.

(11) Aime, S.; Cravotto, G.; Crich, S. G.; Giovenzana, G. B.; Ferrari, M.; Palmisano, G.; Sisti, M. *Tetrahedron Lett.* **2002**, *43*, 783–786.

(12) (a) Facchetti, A.; Abboto, A.; Beverina, L.; Bradamante, S.; Mariani, P.; Stern, C. L.; Marks, T. J.; Vacca, A.; Pagani, G. A. *Chem. Commun.* **2004**, 1770–1771. (b) Andrews, P. C.; Junk, P. C.; Massi, M.; Silberstein, M. *Chem. Commun.* **2006**, 3317–3319. (c) Andrews, P. C.; Beck, T.; Fraser, B. H.; Junk, P. C.; Massi, M. *Polyhedron* **2007**, *26*, 5406–5413. (d) Pietraszkiewicz, M.; Mal, S.; Pietraszkiewicz, O. *Opt. Mater.* **2012**, *34*, 1507–1512.

(13) Rodríguez-Diéguez, A.; Mota, A. J.; Seco, J. M.; Palacios, M. A.; Romerosa, A.; Colacio, E. *Dalton Trans.* **2009**, 9578–9586.

(14) (a) Giraud, M.; Andreiadis, E. S.; Fisyuk, A. S.; Demadrille, R.; Pécaut, J.; Imbert, D.; Mazzanti, M. *Inorg. Chem.* **2008**, *47*, 3952–3954. (b) Andreiadis, E. S.; Demadrille, R.; Imbert, D.; Pécaut, J.; Mazzanti, M. *Chem.—Eur. J.* **2009**, *15*, 9458–9476. (c) Bozoklu, G.; Marchal, C.; Pécaut, J.; Imbert, D.; Mazzanti, M. *Dalton Trans.* **2010**, *39*, 9112–9122. (d) Andreiadis, E. S.; Imbert, D.; Pécaut, J.; Demadrille, R.; Mazzanti, M. *Dalton Trans.* **2012**, *41*, 1268–1277. (e) Wartenberg, N.; Raccurt, O.; Bourgeat-Lami, E.; Imbert, D.; Mazzanti, M. *Chem.—Eur. J.* **2013**, *19*, 3477–3482.

(15) Lin, J.-M.; Guan, Y.-F.; Wang, D.-Y.; Dong, W.; Wang, X.-T.; Gao, S. *Dalton Trans.* **2008**, 6165–6169.

(16) (a) Wu, M.-F.; Wang, M.-S.; Guo, S.-P.; Zheng, F.-K.; Chen, H.-F.; Jiang, X.-M.; Liu, G.-N.; Guo, G.-C.; Huang, J.-S. *Cryst. Growth Des.* **2011**, *11*, 372–381. (b) Liang, L.; Peng, G.; Ma, L.; Sun, L.; Deng, H.; Li, H.; Li, W. *Cryst. Growth Des.* **2012**, *12*, 1151–1158.

(17) D'Allesio, D.; Muzzioli, S.; Skelton, B. W.; Stagni, S.; Massi, M.; Ogdén, M. I. *Dalton Trans.* **2012**, *41*, 4736–4739.

(18) Eulgem, P. J.; Klein, A.; Maggiorosa, N.; Naumann, D.; Pohl, R. W. H. *Chem.—Eur. J.* **2008**, *14*, 3727–3736.

(19) (a) Steinhäuser, G.; Giester, G.; Leopold, N.; Wagner, C.; Villa, M. *Helv. Chim. Acta* **2009**, *92*, 2038–2051. (b) Steinhäuser, G.; Giester, G.; Leopold, N.; Wagner, C.; Villa, M.; Musilek, A. *Helv. Chim. Acta* **2010**, *93*, 183–202.

(20) (a) Steinhäuser, G.; Giester, G.; Wagner, C.; Leopold, N.; Sterba, J. H.; Lendl, B.; Bichler, M. *Helv. Chim. Acta* **2009**, *92*, 1371–1384. (b) Qiao, C.-F.; Wei, Q.; Xia, Z.-Q.; Zhou, C.-S.; Chen, S.-P. *J. Therm. Anal. Calorim.* **2012**, *107*, 527–533.

(21) Steinhäuser, G.; Giester, G.; Wagner, C.; Weinberger, P.; Zachhuber, B.; Ramer, G.; Villa, M.; Lendl, B. *Inorg. Chem.* **2012**, *51*, 6739–6745.

(22) Reviews: (a) Voitekhovich, S. V.; Gaponik, P. N.; Koldobskii, G. I. *Russ. J. Org. Chem.* **2005**, *41*, 1565–1582. (b) Gaponik, P. N.; Voitekhovich, S. V.; Ivashkevich, O. A. *Russ. Chem. Rev.* **2006**, *75*, 507–539. (c) Zhao, H.; Qu, Z.-R.; Ye, H.-Y.; Xiong, R.-G. *Chem. Soc.*

Rev. **2008**, *37*, 84–100. (d) Popova, E. A.; Trifonov, R. E.; Ostrovskii, V. A. *ARKIVOC* **2012**, 45–65.

(23) (a) Wu, L.-L.; Yang, C.-H.; Sun, I.-W.; Chu, S.-Y.; Kao, P.-C.; Huang, H.-H. *Organometallics* **2007**, *26*, 2017–2023. (b) Stagni, S.; Orselli, E.; Palazzi, A.; De Cola, L.; Zacchini, S.; Femoni, C.; Marcaccio, M.; Paolucci, F.; Zanarini, S. *Inorg. Chem.* **2007**, *46*, 9126–9138. (c) Werrett, M. V.; Chartrand, D.; Gale, J. D.; Hanan, G. S.; MacLellan, J. G.; Massi, M.; Muzzioli, S.; Raiteri, P.; Skelton, B. W.; Silberstein, M.; Stagni, S. *Inorg. Chem.* **2011**, *50*, 1229–1241.

(24) Yang, D.; Fokas, D.; Li, J.; Yu, L.; Baldino, C. M. *Synthesis* **2005**, 47–56.

(25) van Es, T. J. *Chem. Soc.* **1965**, 1564.

(26) Chill, S. T.; Mebane, R. C. *Synth. Commun.* **2009**, *39*, 3601–3606.

(27) Finnegan, W. G.; Henry, R. A.; Lofquist, R. J. *Am. Chem. Soc.* **1958**, *80*, 3908–3911.

(28) Latva, M.; Takalo, H.; Mukkala, V. M.; Matachescu, C.; Rodríguez-Ubis, J. C.; Kankare, J. J. *Lumin.* **1997**, *75*, 149–169.

(29) Carnall, W. T.; Fields, P. R.; Rajnak, K. J. *Chem. Phys.* **1968**, *49*, 4450–4455.

(30) Napier, G. D. R.; Neilson, J. D.; Shepherd, T. M. *Chem. Phys. Lett.* **1975**, *31*, 328–330.

(31) Werts, M. H. V.; Jukes, R. T. F.; Verhoeven, J. W. *Phys. Chem. Chem. Phys.* **2002**, *4*, 1542–1548.

(32) Aebischer, A.; Gumy, F.; Bünzli, J.-C. G. *Phys. Chem. Chem. Phys.* **2009**, *11*, 1346–1353.

(33) Brown, I. D.; Altermatt, D. *Acta Crystallogr.* **1985**, *B41*, 244–247.

(34) Trzesowska, A.; Kruszynski, R.; Bartczak, T. J. *Acta Crystallogr.* **2005**, *B61*, 429–434.

(35) (a) Tanner, P. A. *Chem. Soc. Rev.* **2013**, *42*, 5090–5101. (b) Tu, D.; Liu, Y.; Zhu, H.; Li, R.; Liu, L.; Chen, X. *Angew. Chem., Int. Ed.* **2013**, *52*, 1128–1133. (c) Liu, Y.; Tu, D.; Zhu, H.; Chen, X. *Chem. Soc. Rev.* **2013**, *42*, 6924–6958.

(36) Böttger, M.; Wiegmann, B.; Schaumburg, S.; Jones, P. G.; Kowalsky, W.; Johannes, H.-H. *Beilstein J. Org. Chem.* **2012**, *8*, 1037–1047.

(37) (a) Lewis, F. W.; Hudson, M. J.; Harwood, L. M. *Synlett* **2011**, 2609–2632. (b) Kolarik, Z. *Chem. Rev.* **2008**, *108*, 4208–4252. (c) Bremer, A.; Ruff, C. M.; Girnt, D.; Müllich, U.; Rothe, J.; Roesky, P. W.; Panak, P. J.; Karpov, A.; Müller, T. J. J.; Denecke, M. A.; Geist, A. *Inorg. Chem.* **2012**, *51*, 5199–5207.

(38) (a) Singh, R. P.; Gao, H.; Meshri, D. T.; Shreeve, J. M. *Struct. Bonding (Berlin)* **2007**, *125*, 35–83. (b) Klapötke, T. M. *Struct. Bonding (Berlin)* **2007**, *125*, 85–121.